Space-time conditional autoregressive modeling to estimate neighborhood-level risks for dengue fever in Cali, Colombia

Desjardins, M.R.[1*], Eastin, M.D.[2], Paul, R.[3], Casas, I.[4], & Delmelle, E.M.[2]

[1]Spatial Science for Public Health Center, Department of Epidemiology, Johns Hopkins Bloomberg School of Public Health, Baltimore, MD, 21205
[2]Department of Geography and Earth Sciences & Center for Applied Geographic Information Science. University of North Carolina at Charlotte, Charlotte, NC 28223
[3]Department of Public Health Sciences, University of North Carolina at Charlotte, Charlotte, NC 28223
[4]Louisiana Tech University, School of History and Social Sciences, Ruston, LA 71272
*Corresponding author: mdesjar3@jh.edu; +1 (203) 233-5381; 627 N. Washington St., Baltimore, MD, 21205

Abstract.
Vector-borne diseases (VBDs) affect more than 1 billion people a year worldwide, cause over 1 million deaths, and cost hundreds of billions of dollars in societal costs. Mosquitoes are the most common vectors, responsible for transmitting a variety of arboviruses. Dengue fever (DENF) has been responsible for nearly 400 million infections annually. Dengue fever is primarily transmitted by female *Aedes aegypti* and *Aedes albopictus* mosquitoes. Since both *Aedes* species are peri-domestic and container-breeding mosquitoes, dengue surveillance should begin at the local level - where a variety of local factors may increase the risk of transmission. Dengue has been endemic in Colombia for decades and is notably hyperendemic in the city of Cali. For this study, we use weekly cases of DENF in Cali, Colombia from 2015-2016; and develop space-time conditional autoregressive models to quantify how DENF risk is influenced by socioeconomic, environmental, and accessibility risk factors, and lagged weather variables. Our models identify high-risk neighborhoods for DENF throughout Cali. Statistical inference is drawn under Bayesian paradigm using Markov Chain Monte Carlo techniques. The results provide detailed insight about the spatial heterogeneity of DENF risk and the associated risk factors (such as weather, proximity to *Aedes* habitats, and socioeconomic classification) at a fine-level, informing public health officials to motivate at-risk neighborhoods to take an active role in vector surveillance and control, and improving educational and surveillance resources throughout the city of Cali.

Keywords: Space-time modeling, spatial epidemiology, vector-borne disease, urban health

Funding: This research was funded by a 2019 American Association of Geographers (AAG) Dissertation Research Grant and a 2019 UNC-Charlotte Graduate School Summer Fellowship.

1. Introduction

Vector-borne diseases, more specifically mosquito-borne arboviruses are responsible for 1 billion infectious disease cases each year, globally[1,2]. Mosquitoes transmit a variety of arboviruses and are the most common vectors. Dengue fever (DENF) is a mosquito-borne disease that is responsible for the majority of the global burden of arboviruses[3]. Over 40% of humans are at risk of transmission, with incidence rising 30-fold in the last 50 years; and it is estimated that there are approximately 390 million DENF infections annually[4]. DENF is primarily transmitted by the *Aedes aegypti* and *Aedes albopictus* mosquitoes[5,6]. Both species are container-breeding mosquitoes that have become prolific in urban areas due to the widespread availability of breeding habitats[7].

Dengue is a flavivirus that causes DENF and there are four serotypes that follow the human cycle[8]. The incubation period ranges from 3-14 days after being bit by an infected mosquito, and symptoms can last from 2-7 days[9], however, approximately 80% of infected individuals are asymptomatic. Infection from one serotype will result in lifelong immunity to that serotype, however, secondary infection with another serotype can lead to severe forms of DENF[10], such as dengue hemorrhagic fever (DHF) and dengue shock syndrome (DSS). DHF and DSS primarily affects pediatric patients, but it has also been found among adults (especially the elderly); and mortality from dengue is highest among children and those who have experienced DSS[11].

It is critical to implement surveillance strategies that can improve the understanding of DENF transmission. Improving DENF surveillance can facilitate the timely reporting of disease cases, reduce underreporting, inform policymakers, increase disease awareness, define funding and research priorities[12]; ultimately reducing the economic and public health burden in at-risk

locations around the world[13]. Approaches and advances in geographic information science (GIScience) and spatial epidemiology play critical roles in DENF surveillance – such as tracking diffusion and cyclic patterns, detecting clusters and mapping disease rates and risk[14] and understanding the place-based determinants of disease transmission[15]. DENF risks and rates will vary by place and covariate data are needed to identify significant variables responsible for observable spatial patterns[16].

Therefore, it is critical to examine the social, economic, environmental, biological, and institutional factors that may affect DENF prevalence in a particular area. Urban regions are highly complex, and neighborhoods are the scale that public health departments most effectively operate[17]. Therefore, more small-area studies in spatial epidemiology are required to effectively uncover the spatial and temporal heterogeneity of DENF rates across urban landscapes at these fine levels of granularity. For example, education, income, age, access to care, and quality of prevention strategies are known to strongly influence an individual's susceptibility to VBDs[18,19]. Likewise, the dynamics of how temperature, precipitation, and humidity affect vector abundance and DENF transmission are critical to developing and implementing effective sub-seasonal risk model[20] and long-term mitigation in response to climate change[21].

Conditional autoregressive (CAR) models can be utilized to examine how DENF risk is influenced by socioeconomic, environmental, and accessibility risk factors, and lagged weather variables. For example, a particular location may be influenced by DENF rates and a variety of explanatory variables (e.g. socioeconomic status, proximity to *Aedes* habitats, etc.) contained in surrounding locations (spatial spillover/diffusion effects). CAR models can be fitted to data under Bayesian paradigm (i.e. relying on prior beliefs/borrowing information to inform future estimations) using – Bayesian hierarchical models (BHM), which are widely used techniques in

92 geography and public health to model spatial and spatiotemporal data[22]. In short, BHMs can
93 model complicated spatial and space-time processes by conditionally modeling the variations in
94 data, the process, and unknown parameter[23]. The temporal extension – ST-CAR can estimate the
95 value of a variable (e.g. disease rates) at a particular location and time, which will be related to
96 current and past values of the surrounding locations and time periods; essentially testing for
97 spatiotemporal dependence. ST-CAR models have been used to study the effect of air pollution
98 on human health[24], substance abuse and its relationship with child abuse[25], influenza[26], and
99 DENF[27,28,29].

100 More research is necessary to examine the local variations in DENF transmission
101 dynamics at very fine spatial and temporal scales. Delmelle et al. (2016)[30] used a geographically
102 weighted regression (GWR[31]) model which identified six significant socioeconomic and
103 environmental independent variables (including proximity to tire shops and population density)
104 of DENF rates in Cali, Colombia at the neighborhood-level. However, the explanatory power of
105 GWR and its temporal extension – GTWR[32]), is limited. Both CAR and ST-CAR models
106 produce model-based estimates and inference derived from varying effects via spatial random
107 fields – e.g. borrowing strength from neighborhood spatial and temporal proximity; while GWR
108 models allow the covariates to vary in space (and time in the case of GTWR), but inference is ad
109 hoc. In other words, ST-CAR models can estimate spatially and temporally varying associations
110 between the dependent (e.g. disease rates) and independent variables based on locally weighted
111 regressions in both geographic and attribute space; while GTWR can only produce local
112 estimates in geographic space. It is therefore worthwhile to utilize ST-CAR modeling in small-
113 area DENF studies at fine temporal scales.

This study utilizes a ST-CAR modeling approach to examine the influence of socioeconomic, environmental, weather and climate variables on DENF outbreaks in Cali, Colombia at the neighborhood- and weekly levels between 2015 and 2016. The approach can determine if DENF rates and covariates in one neighborhood are influenced by rates and covariates in surrounding neighborhoods and time periods. We also estimate disease risks using temporally lagged weather variables. Our modeling approach is capable of identifying regions with high risk clusters at the neighborhood-level. The results provide detailed insight about the spatial heterogeneity of disease risk and the associated risk factors at a fine-level; informing public health officials to motivate at-risk neighborhoods to take an active role in vector surveillance and control, and improving educational and surveillance resources throughout the city of Cali.

The remainder of this paper is as follows: section 2 provides information about Cali, the DENF cases, and candidate independent variables, the technique to select the lagged weather variables, and the ST-CAR modeling approach. Section 3 provides the modeling results, including maps of the estimated DENF rates by week for each neighborhood in Cali. Section 4 discusses key findings, strengths, limitations, and avenues of future research; and section 5 summarizes findings with concluding remarks.

2. Data & Methods

2.1 Study Area & Data

Cali is the second-largest city in Colombia and third most populous with an estimated 2010 population of 2.3 million (average density of 4,000 km^2). The city is comprised of 340 neighborhoods (Spanish - barrios), which are classified by socioeconomic stratum (ranging from 1-6); where a ranking of 1-2 is low, 3-4 is middle, and 5-6 is high. The classifications are

137 defined by the external physical characteristics of the dwelling, its immediate surroundings, and
138 its urban context. For example, urban context includes variables such as poverty, social
139 deviation, urban decay, industry, commercial; immediate surroundings include access roads,
140 sidewalks; and the characteristics of the dwelling include front lawn, garage, façade material,
141 door material, front of the house dimensions, and windows (income is not considered). This
142 stratification is only applied to residential constructions[33]. Figure 1 provides a map of
143 neighborhoods in Cali and their corresponding ranking. The average size of neighborhoods in
144 Cali is 0.35 square kilometers. Some of the smaller neighborhoods are in the city core, which is
145 where the city was founded. The largest neighborhood is to the south and corresponds to newer
146 developments and is an area that houses three of the largest universities in Cali.
147 Individual cases of DENF for the years of 2015 and 2016 at the weekly level were used
148 (Figure 2 - top), which were provided by Colombia's National Institute of Health. Between 2015
149 and 2016, Cali experienced three major outbreaks: March to mid-May 2015; February to early-
150 April 2016; and mid-June 2016 to early August 2016 (represented by the peaks in Figure 2 - top).
151 The cases were geocoded to the neighborhood level using each neighborhood's name as the
152 address locator in the geocoder algorithm in ArcGIS 10.6 (ESRI, Redlands, CA) Each DENF
153 case record contained a neighborhood where the infected individual lived (individual addresses
154 were not available), then the geocoder aggregated the cases to a particular neighborhood after a
155 successful match. As a result, 26,503 out of 35,498 DENF cases (74.6%) were successfully
156 geocoded and aggregated to the neighborhood-level in Cali. Cases that were not geocoded did
157 not have an address nor a neighborhood, therefore, it was impossible to assign coordinates to the
158 unmatched cases.

Figure 2 (bottom) provides a map of the total DENF cases per neighborhood between 2015 and 2016 in Cali. The eastern portion of Cali observed the highest number of DENF cases between the two years in our study period. These neighborhoods were majority low strata (1 and 2); however, there are numerous middle strata (3 and 4) neighborhoods in the central and southern portions of Cali with a high number of DENF cases. There are also high strata neighborhoods with a high proportion of cases in the central and western regions of Cali, especially those that are adjacent to lower strata neighborhoods.

[Insert] Figure 1. Neighborhoods in Cali, Colombia and their ranking by socioeconomic strata (1-6).

[Insert] Figure 2. Temporal distribution of weekly DENF cases in Cali from January 2015 through December 2016 (top); spatial distribution of DENF rates per 1,000 for the study period (bottom).

The socioeconomic and demographic data were provided by the Colombian census (either 2005 or 2010 estimates provided by the City of Cali), including population density, age, race, households with sewer and water access, educational attainment, employment status, socioeconomic stratum, among others. The last national census occurred in 2005, while the new 2018 census has yet to be released. The location of healthcare centers and the environmental variables were provided by the city of Cali (2010 data) – green zones, rivers, tire shops, water pumps, cemeteries, and plant nurseries, which were geocoded as point layers with the exception of green zones (area - polygons) and rivers (lines). The environmental variables are included as potential *Aedes* habitats. For green zones, the area of the green zones for each neighborhood was computed in square-kilometers. Similar to Delmelle et al. (2016)[30], relative proximity to rivers, tire shops, water pumps, cemeteries, plant nurseries, and healthcare centers was computed by using kernel density estimation (KDE) – representing the density of points for each layer. KDE

was also computed to produce the density of trees. Zonal statistics in ArcGIS 10.6 was used to summarize the average KDE for each neighborhood in Cali.

Finally, the weather variables selected for evaluation (Table 1) are consistent with current understanding of how weather conditions impact *Aedes* survival, abundance, and behavior, including viral transmission rates[34,20] (Table 5). Given our goal of developing a risk model using 2015-16 weekly-level DENF data, the weather variables entail weekly summaries of 2014-16 daily meteorological observations collected at the Cali international airport and obtained from the Global Historical Climate Network archive[35] maintained by the National Centers for Environmental Information (http://www.ncdc.noaa.gov). All weekly weather variables were computed following the methods outlined in Eastin et al. (2014)[20], and summary statistics for the 2014-16 period are provided in Table 1. A total of 49 candidate predictor variables of DENF were evaluated in this study (Table 1). Due to the differences in units of measurements, each variable was normalized between 0 and 1 (i.e., between the maximum and minimum values listed in Table 1) for all subsequent analyses.

206 **Table 1: Descriptive Statistics of the Candidate Independent Variables for Cali, Colombia**
207 **(# *Mean; **Median; Total***)**

Variable ID	Variable Name	Year	Source	Value#	Range
Environmental/*Aedes* Habitats					
Green	Area of green zones (km^2)	2010	City of Cali	196.4***	0-34.9
Rivers	Relative proximity to river	2010	City of Cali	1082.0	0-9,3539.3
Tires	Relative proximity to tire shops	2010	City of Cali	5.1*	0-28.6
WPumps	Relative proximity to water pumps	2010	City of Cali	0.1*	0-0.5
Cemet	Relative proximity to cemeteries	2010	City of Cali	2.1*	0-9.8
PNurseries	Relative proximity to plant nurseries	2010	City of Cali	0.5*	0-1.9
Trees	Density of trees (km^2)	2010	City of Cali	1,698.9***	8.6-6,355.6
Healthcare Accessibility					
DistHealth	Relative proximity to a healthcare center	2010	City of Cali	4.4*	0-9.2
HealthAvg	Mean healthcare center density (km^2)	2010	City of Cali	4.2*	0-74.4
Socioeconomic & Demographic					
Strata	Neighborhood Stratum	2010	Census	3**	1-6
Popdens	Population density (km^2)	2005	Census	22,099*	0-56,814
%OHH	Density of occupied households (km^2)	2005	Census	837.2*	0-14,885
%UHH	Density of unoccupied households (km^2)	2005	Census	98.6*	0-688.4
%Sew	Households with sewer (%)	2005	Census	89.8*	0-100
%Water	Households with water (%)	2005	Census	90.2*	0-100
%A04	Individual age 0-4 years old (%)	2005	Census	7.3*	0-15.7
%A514	Individual age 5-14 years old (%)	2005	Census	17.2*	0-27.8
%A1524	Individual age 15-24 years old (%)	2005	Census	17.5*	0-69.2
%A2539	Individual age 25-39 years old (%)	2005	Census	23.4*	0-39.1
%A4064	Individual age 40-64 years old (%)	2005	Census	26.3*	0-47.8
%A65	Individual age 65 years old or more (%)	2005	Census	8.3*	0-23.4
%Fem	Female population (%)	2005	Census	53.4*	0-100
%White	White population (%)	2005	Census	77.2*	0-96.7
%Black	Black population (%)	2005	Census	22.1*	0-70.6
%Indig	Indigenous population (%)	2005	Census	0.5*	0-8.7
%Disabled	Individuals with disabilities (%)	2005	Census	1.1*	0-5.7
%NoRW	Individuals who cannot read/write (%)	2005	Census	6.8*	0-5.7
%NoEduc	Individuals with no education (%)	2005	Census	3.6*	0-16.8
%LowEduc	Individuals with low education (%)	2005	Census	26.9*	0-52.8
%MedEduc	Individuals with medium education (%)	2005	Census	49.6*	0-71.3
%HighEduc	Individuals with high education (%)	2005	Census	19.9*	0-56.0
%Work	Employed individuals (%)	2005	Census	41.1*	0-58.9
%Unem	Unemployed individuals (%)	2005	Census	1.5*	0-10.3
%Retired	Retired individuals (%)	2005	Census	3.9*	0-15.9
%HW	Individuals doing housework (%)	2005	Census	13.6*	0-18
%Students	Students (%)	2005	Census	22.9*	0-36.8
%Married	Married individuals (%)	2005	Census	19.0*	0-37.9
%Single	Single individuals (%)	2005	Census	38.9*	0-100
Weather (Weekly Observations)					
Tavg	Mean Temperature of (°C)	2014-2016	City of Cali	24.2*	22.5-25.7
Tmax	Mean Maximum Temperature (°C)	2014-2016	City of Cali	31.2*	28.5-34.2
Tmin	Mean Minimum Temperature (°C)	2014-2016	City of Cali	19.4*	17.2-20.7
DTRavg	Mean Daily Temperature Range (°C)	2014-2016	City of Cali	11.8*	9-15.7
DTRmax	Maximum Daily Temperature Range (°C)	2014-2016	City of Cali	14.3*	10.6-21
RHavg	Mean Relative Humidity (%)	2014-2016	City of Cali	73.3*	63.9-83.7
RHrng	Relative Humidity Range (%)	2014-2016	City of Cali	10.6*	2.7-24.1
RainT	Total Rain (mm)	2014-2016	City of Cali	12.3*	0-103
RainD	Total Days with Measurable Rainfall	2014-2016	City of Cali	2.8*	0-7
CoolD	Days with Minimum Temperature < 18 (°C)	2014-2016	City of Cali	0.6*	0-5
WarmD	Days with Maximum Temperature > 32 (°C)	2014-2016	City of Cali	2.0*	0-7

208

2.2 Methodology

2.2.1 Principal component analysis & VIF testing

Due to the large number of socioeconomic, demographic variables, and environmental variables (n = 36), we utilized Variance Inflation Factor (VIF)[36] testing and a principal component analysis (PCA[37]) in Stata. We did not include all variables in the PCA because we wanted to interpret particular independent variables of DENF individually, which is important for potential decision-making. For example, identifying the effects of individual *Aedes* habitats (e.g. tire shops and trees) can provide more intuitive results than grouping them in a PCA. As a result five variables were selected for subsequent modeling with a VIF value < 3: population density, tree density, relative proximity to rivers, relative proximity to tire shops, and relative proximity to plant nurseries.

The PCA's purpose is to reduce and simplify the variables into new variable (components) that explain a large degree of variation without collinearity between the components. Tables 2 and 3 provide the results of the PCA analysis and include the variables that were included – which were not included in the VIF testing. Table 2 describes the variance explained by the top three principal components and Table 3 shows the variables that belong to each component. After examining the eigenvalues and component loadings with coefficients > 0.40, the first two components were selected for inclusion in the space-time modeling, which explains 60.8% of the variance (42% and 18.8%, respectively).

PC1 is strongly associated with (correlation close to 0.5 and above) neighborhood strata, individuals who are employed, retired persons, married individuals, empty households, and individuals with high education. PC2 mainly explains occupied households, individuals who do housework, and individuals who are students. PC3 explains the combined effect from disabled individuals but was excluded from further analysis and it was included as a separate variable in

233 further VIF (variance inflation factor) testing with the remaining covariates. PC1 can be
234 interpreted as employed, higher-income people who are likely to be older and married due to the
235 large coefficients of retired and married individuals. PC2 can be interpreted as people who are
236 likely to spend more time at home than those in PC1 because they are either students or do
237 housework for a living. PC2 probably also captures younger individuals due to the inclusion of
238 students.

239 **Table 2. Explained variance by top three principal components**

Component	Extraction Sums of Squared Loadings			Rotation Sums of Squared Loadings	
	Total	Variance	Cumulative %	Total	% of Variance
1	4.516	45.163	45.163	4.203	42.032
2	1.703	17.031	62.194	1.882	18.817
3	1.072	10.719	72.912	1.206	12.064

240

241 **Table 3. Rotated component loadings with coefficient > 0.40**

Variable	Component		
	1	2	3
Strata*	.856		
% OHH**		.749	
% HW**		.657	
% Work**	.784		
% Retired**	.781		
% Disabled**			.782
% Student**		.873	
% Married**	.941		
% EmptyHH**	.484		-.514
% HighEduc**	.940		

*Neighborhood strata classification between 1 and 6.

**proportion (%) of individuals in each category: (1) Occupied Households (2) Work from Home (3) Retired persons (4) Disabled persons (5) Students (6) Married persons (7) Empty Households (8) holds college degree or higher

2.2.2 Selecting Lagged Weather Variables

First, VIF testing was used to assess multicollinearity among the candidate weekly weather variables (Table 1) and remove the most inter-correlated variables while retaining the most independent. Seven variables (with VIF values < 3) were selected for the subsequent cross-correlation analysis: Tavg, DTRmax, RHrng, RainT, RainD, CoolD, and WarmD. Next, lagged cross-correlations were computed between weekly DENF rates and each weather variable over an 8-week window (Table 4). Such time frame was considered the most biologically plausible based on existing literature of how weather affects the full vector lifecycle and viral transmission dynamics[20,34] (see Table 5). Finally, an optimal lag for each weather variable was selected among those weeks exhibiting a statistically significant (at the 5% level; adjusted for multiple testing) cross-correlation within the 1-8 week lag window (0-week lags were not considered due to their lack of predictive potential). For six variables (Tavg, DTRmax, RainT, RainD, CoolD, WarmD), the selected optimal lags (5-weeks, 5-weeks, 3-weeks, 5-weeks, 2-weeks, 5-weeks, respectively) exhibited the maximum cross-correlation coefficient (Table 4). For RHrng, the maximum correlation occurred at 6-weeks, but the 3-week lag was deemed optimal since existing literature suggests that relative humidity is most influential on adult vectors and the gonotrophic cycle (Table 5). The optimal lags were included in the ST-CAR models.

Table 4. Lagged cross-correlations between DENF rates and weekly weather variables during

2015-2016 in Cali, Colombia

Lag (Weeks)	Tavg	RainT	RHrng	DTRmax	RainD	CoolD	WarmD
0	0.419*	-0.207	-0.012	0.463*	-0.508*	0.202	0.507*
-1	0.285*	-0.413*	-0.057	0.150	0.011	-0.109	0.261*
-2	0.032	0.098	0.212	0.077	0.337*	-0.354**	0.095
-3	0.074	-0.458**	-0.448**	0.029	-0.012	-0.166	-0.012
-4	0.257*	-0.092	-0.166	0.105	-0.488*	0.081	0.201
-5	0.369**	-0.262*	-0.362*	0.236**	-0.542**	0.201	0.287**
-6	0.255*	-0.316*	-0.557*	-0.104	-0.359*	0.304*	0.014
-7	0.221	-0.011	-0.473*	0.079	-0.338*	0.283*	-0.047
-8	0.242	-0.315*	-0.098	-0.088	-0.309*	0.181	-0.156

*Significant at the 5% level (after adjustment via a Bonferroni correction for multiple testing)
**Selected Lag for ST-CAR modeling

278 **Table 5. Temporally-lagged weather variables & correlation with *Aedes*' life cycle (*Based on 20, 34); #Total lag (weeks prior to lab**
279 **confirmation) - accumulated range for each stage in the vector-dengue transmission cycle**

Development Stage	Range (Days) *	Total Lag (Weeks) #	Variable	Expected Relation	Rationale	Primary Sources
Larval/Pupa Development (vector grows in water)	10-21	**3-8**	RainT	Positive	More total rain produces more stagnant pools; promotes larval development	38, 39
			RainD	Positive	More frequent rain produces more stagnant pools; promotes larval development	40, 41
			Tavg	Positive	Warmer temperatures promote larval development	42, 43
			DTRmax	Negative	Smaller ranges imply fewer hours with cold temperatures; greater larval survival	20, 44
			RHrng	Negative	Smaller ranges imply fewer dry days; stagnant pools quickly evaporate	20, 45
			WarmD	Positive	More warmer days promote greater larval densities	44, 46
			CoolD	Negative	Fewer cold days promote greater larval survival	44, 46
Gonotrophic Cycle (vectors feed on humans)	3-7	**2-5**	RainT	Negative	Rainfall tends to coincide with cooler temperatures; less vector feeding	20, 47
			RainD	Negative	Rainfall tends to coincide with cooler temperatures; less vector feeding	20, 47
			Tavg	Positive	Vector feeding more frequent at warmer temperatures	48, 49
			DTRmax	Negative	Vector feeding more frequent at warmer temperatures; smaller DTRmax implies fewer cold hours	20, 42
			RHrng	Positive	Vector feeding more frequent during dry periods; larger RHrng implies more dry days	20, 45
			WarmD	Positive	Vector feeding more frequent at warmer temperatures	50
			CoolD	Negative	Vector feeding more frequent at warmer temperatures; fewer cold hours	50
Extrinsic Incubation (virus matures in vector)	7-15	**1-4**	RainT	Unknown	No known link between rainfall and extrinsic incubation	N/A
			RainD	Unknown	No known link between rainfall and extrinsic incubation	N/A
			Tavg	Positive	Viral development more rapid at warmer temperatures	48, 51
			DTRmax	Negative	Viral development more rapid at warmer temperatures; smaller DTRmax implies fewer cold hours	50
			RHrng	Positive	Viral development more rapid in humid environments; smaller RHrng implies fewer dry days	52, 53
			WarmD	Positive	Viral development more rapid at warmer temperatures	50
			CoolD	Negative	Viral development more rapid at warmer temperatures; fewer cold hours	50
Intrinsic Incubation (virus matures in humans)	1-12	**0-2**	N/A	N/A	No known link between weather and intrinsic incubation	N/A
Dengue Reported (lab confirmation)	---	**---**	N/A	N/A	N/A	N/A
Total	21-55	**0-8**				

2.2.3 Poisson GLMs

First, a Poisson generalized linear model (GLM) is computed to detect significant effects of independent variables on a dependent variable (DENF risk); and the presence of spatiotemporal autocorrelation in the residuals. The Poisson GLM is defined as:

$$Y_{ij} \sim Poisson\,(E_{ij}R_{ij}) \tag{1}$$

$$\begin{aligned}\log(R_{ij}) = {} & \beta_0 + \beta_1 PC1_i + \beta_2 PC2_i + \beta_3 PNurseries_i + \beta_4 Tires_i \\ & + \beta_5 popdens_i + \beta_6 rivers_i + \beta_7 trees_i + \beta_8 Tavg_{ij} \\ & + \beta_9 DTRMax_{ij} + \beta_{10} RHrng_{ij} + \beta_{11} RainT_{ij} + \beta_{12} RainD_{ij} \\ & + \beta_{13} CoolD_{ij} + \beta_{14} WarmD_{ij}\end{aligned} \tag{2}$$

where Y_{ij} is the observed DENF count in neighborhood *i* at week *j*; E_{ij} is the expected DENF count in neighborhood *i* at week *j*; and R_{ij} is the disease risk in neighborhood *i* at week *j* (see supplemental materials for the results of the Poisson GLM).

Global Moran's I[54] was then computed to detect spatial autocorrelation of the Poisson GLM residuals for each time period. Essentially, the Global Moran's I test determines if there is evidence of unexplained spatial autocorrelation in the residuals; and if positive spatial autocorrelation is detected, then the assumption of independence is not valid for the data, and spatiotemporal autocorrelation should be considered when estimating covariate effects on the dependent variable. The global Moran's I index ranges from -1 to 1, while -1 indicates strong negative spatial autocorrelation, 0 indicates complete spatial randomness, and 1 indicates strong positive spatial autocorrelation; and the statistic is defined as:

$$I = \frac{n \sum_i \sum_l w_{il}(x_i - \bar{x})(x_l - \bar{x})}{\sum_i \sum_l w_{il} \sum (x_i - \bar{x})^2} \tag{3}$$

where *n* is the total number of neighborhoods, w_{il} is the spatial weight between neighborhood *i* and *l*, $\bar{x}$ is the mean of residuals for all neighborhoods, $x_i$is the residual value in neighborhood *i*,

297 and x_l is the residual in neighborhood *l*. The Moran's I tests were conducted in RStudio 1.2.5
298 with R version 3.6.

299 2.2.4 ST-CAR Modeling

300 Next, a Bayesian hierarchical model[24,25] is defined using a Poisson data model (for
301 case/population data). The model "represents the spatio-temporal pattern in the mean response
302 with a single set of spatially and temporally autocorrelated random effects. The effects follow a
303 multivariate autoregressive process of order 1[54]. In other words, when going from one week to
304 another (e.g. j +1), it will yield an effect on the dependent variable (DENF risk). Therefore, this
305 model examines linear trends which can be interpreted as how DENF risk is influenced across
306 time.

307 It is assumed that the estimated effect on DENF risk in the ST-CAR model is not specific
308 to a particular week, but a process that is influenced by the covariate data across the weeks
309 (temporal unit). Suppose a study region is divided into a collection of N non-overlapping areal
310 units (e.g. neighborhoods) indexed by $i \in \{1\ldots,N\}$; and the data is observed for multiple time
311 periods, that is: $j \in \{1\ldots,T\}$. As suggested before, ST-CAR models utilize prior distributions,
312 where the CAR distributions state that adjacent variables in space or time are conditionally
313 autocorrelated, and non-adjacent variables are conditionally independent. The spatial weight
314 matrix is defined as: $W = (w_{ik})$, where a value of 1 indicates that i and k are spatially adjacent,
315 and 0 otherwise. Since it is unknown where a person was infected, the abovementioned
316 adjacency matrix is a proxy for *Aedes'* maximum range – since they do not fly more than 400
317 meters from where they emerged as larvae[10]. A temporal weight matrix can also be defined as D
318 $= (d_{jt})$, where a value of 1 is given if $t - j = 1$, and 0 otherwise. The first part of the model is
319 defined as:

$$Y_{ij}|E_{ij,}R_{ij} \sim Poisson(E_{ij}R_{ij}) \quad 4)$$

$$\ln(R_{ij}) = X_{ij}^{T}\beta + O_{ij} + \phi_{ij} \quad 5)$$

$$\beta_k \sim N(0, 1000)\ k \in \{1, \ldots, p\}, \quad 6)$$

where Y_{ij} is the observed DENF count in neighborhood *i* at week *j*; E_{ij} is the expected disease count in neighborhood *i* at week *j*; and R_{ij} is the disease risk in neighborhood *i* at week *j*. X_{ij}^{T} $(x_{ij1\ldots\ldots}, x_{ijp})$ is a vector of known covariates *p* for neighborhood *i* and week *j*. The parameter β is an associated *p* x 1 vector of regression parameters, which can come from the initial Poisson GLM in Equations 1 and 2. The term O is a vector of known offsets $(O_1, \ldots\ldots, O_N)_{K*N}$, where O_j is a *K* * 1 column vector of offsets (expected DENF cases) for week *j* $(O_{1j}, \ldots\ldots, O_{Kj})$. An offset variable is used to scale the modeling of the mean in Poisson regression with a log link, which is the case in the above model. For example, since the dependent variable is rates, the offset can enforce that 10 cases of DENF in one week is not the same magnitude as 10 cases of DENF in 6 weeks. The parameter ϕ_{ij} denotes spatiotemporally autocorrelated random effects for neighborhood *i* and week *j*. A variety of spatiotemporal structures can be fit for ϕ_{ij}. Here, we use a model that estimates the evolution of the spatial response surface over time without forcing it to be the same for each time period (Rushworth et al. 2014).

$$f(\phi_{1,\ldots,}\phi_T) \sim f(\phi_1)\prod_{j=2}^{T} f(\phi_j|\phi_{j-1}) \quad 7)$$

Where $\phi_j = \left(\phi_{1j,\ldots,\phi_{Nj}}\right)$ is a vector of random effects for week *j*. Temporal autocorrelation is enforced because ϕ_j depends on ϕ_{j-1}. $f(\phi_1)$ enforces spatial autocorrelation in the random effects, where the spatial structure is defined in the CAR prior in Equation 8:

$$\phi_{i1}|\phi_{-i} \sim N\left(\frac{\rho\sum_{k=1}^{N} w_{ik}\phi_{k1}}{\rho\sum_{k=1}^{N} w_{ik} + 1 - \rho}, \frac{\tau^2}{\rho\sum_{k=1}^{N} w_{ik} + 1 - \rho}\right) \quad (8)$$

Where ρ controls the spatial autocorrelation with ρ = 1 indicating strong spatial autocorrelation, which is conditional upon the mean random effects of adjacent neighborhoods. ρ = 0 represents independent random effects with a constant mean and constant variance. The conditional precision is controlled by τ, where precision is higher when more prior information (e.g. adjacent neighborhoods) is borrowed to determine the posterior estimates. Equation 9 (CAR Prior) enforces temporal autocorrelation in the random effects and is defined as:

$$\phi_j|\phi_{j-1} \sim N(\alpha\phi_{j-1}, \tau^2 Q(\rho, W)^{-1})\ j \in \{2,\ldots,T\}, \quad (9)$$

Where $Q(\rho, W)$ is a precision matrix, that is defined as ρ(diagonal(W1) – W) + (1 – ρ)*I*, where *I* is a N x N identity matrix and the '1' is a vector of ones (N x 1). The α controls the temporal autocorrelation, where 0 is temporally independent and 1 is strong temporal dependence. The CAR priors also include weakly informative hyperpriors (i.e. probability distribution from priors to inform/update posterior values), which are the three parameters defined below:

$$\tau \sim \textit{Uniform}\ [0,1000],$$
$$\alpha \sim \textit{Uniform}\ [0,1],$$
$$\rho \sim \textit{Uniform}\ [0,1]$$

The values of the hyperpriors are selected in a way so that our Bayesian inferences are robust and not sensitive to these choices. For example, a non-stationary spatial process would occur when ρ = 1; and non-stationary temporal process would occur if α = 1. Overall, the ST-CAR

model states that when going from one week to another ($j + 1$), it yields an effect on the dependent variable (DENF risk), which is influenced by spatially and temporally dependent covariates. In other words, DENF risk in a target neighborhood is influenced by current and past values of DENF risk and covariates at surrounding neighborhoods and time periods (which is a process that evolves over time). Conceptually, a spatial example would suggest that a neighborhood with low risk of DENF would have an increased risk of DENF if an adjacent neighborhood reported a high risk of DENF (dependence/autocorrelation).

Statistical inference is derived from Markov Chain Monte Carlo (MCMC) simulations[56]. MCMC is a popular technique for Bayesian inference when posterior distributions are not available in closed forms. We used MCMC to generate samples from the posterior distributions induced by our ST-CAR models and used them for parameter and density estimation. For this study, we selected 220,000 MCMC samples; initial 20,000 samples are removed as burn-in; and the thinning parameter is set to 10 (keeping every 10^{th} value and removing all others), which thins the samples to reduce autocorrelation of the Markov Chain. As a result, 20,000 samples are used for statistical inference. The deviance information criterion (DIC) was used for model assessment and comparison, where lower values of DIC indicate a better model fit. The results of two models are presented in section 3: Model 1 (DENF with no lags); Model 2 (DENF with lagged weather variables). Using CARBayesST[24] in R, the two Poisson GLM models (DENF with no lags; DENF with lags) were each fitted to the ST-CAR model described above.

3. Results

3.1 ST-CAR Results

The following subsections contain summaries of model results; relative risk estimates for each independent variable; and mapping the posterior estimates of DENF rates in Cali for particular time periods (temporal cross-sections).

3.1.1 Model 1

Table 6 (left) summarizes the results of Model 1 (DENF with no lags). The 95% credible intervals do not contain a value of 0, indicating that all the covariates exhibit influential relationships with DENF risk at the neighborhood level in Cali between January 2015 and December 2016. The spatial autocorrelation value of 0.98 indicates that there is very strong spatial dependence of the data after adjusting for covariate effects. The temporal autocorrelation value of 0.11 suggests that there is some presence of temporal dependence of the data after adjusting for covariate effects. Therefore, DENF risk in Cali at the neighborhood level is influenced by DENF rates and covariates in surrounding neighborhoods and time periods (weeks). Table 6 (left) also shows the relative risk estimates (%) of DENF in Cali between January 2015 and December 2016. The results suggest a 4.7% increase in DENF risk for PC1; a 4.7% decrease for PC2; a 12.9% increase for proximity to plant nurseries; a 5.5% increase for proximity to tire shops; a 1.5% decrease for population density; a 11.6% decrease for proximity to rivers/ravines; a 36% increase for tree density; a 635% increase for average temperature; a 26.6% increase for days with maximum temp. > 32 °C; a 139% increase for relative humidity range; a 45.8% decrease for total rainfall; a 16.8% decrease for total rain days; a 76.4% increase for cool days; and a 73.6% decrease for warm days when adjusted for other variables. The results will be further explained in the discussion.

Table 6: ST-CAR Model Results (Model 1 – no lags); (Model 2 – lagged weather variables)

	Model 1 – DIC: 67,055.98				Model 2 – DIC: 66,954.16			
	2.50%	**Median**	**97.50%**	**RR (%)**	**2.50%**	**Median**	**97.50%**	**RR (%)**
Intercept	-2.0296	-1.6427	-1.3183	NA	-0.8195	-0.5423	-0.3055	NA
PC1	0.0159	0.0463	0.0785	4.7	0.0459	0.0732	0.1	7.6
PC2	-0.0885	-0.0475	-0.0068	-4.6	-0.0042	0.0382	0.0798	3.9
Pnurseries	0.0203	0.1213	0.2215	12.9	0.0841	0.1806	0.2787	19.8
Tires	-0.0838	0.0531	0.1902	5.5	-0.023	0.1118	0.2469	11.8
Popdens	-0.173	-0.0146	0.1482	-1.5	-0.3296	-0.1749	-0.0176	-16
Rivers	-0.2473	-0.1233	-0.0029	-11.6	-0.2532	-0.1381	-0.0227	-12.9
Trees	0.1254	0.3071	0.4909	36	0.0901	0.2626	0.4404	30
Tavg(L5)	1.5864	1.9947	2.3546	635	-0.6022	-0.2908	0.0415	-25.2
DTRMax(L4)	-0.24	0.2361	0.9014	26.6	0.4579	0.8115	1.2709	125.1
RelHRng(L3)	0.4641	0.8713	1.342	139	0.4317	0.615	0.8213	85
RainT(L3)	-1.3716	-0.613	0.003	-45.8	-2.8222	-2.4343	-2.0671	-91.2
RainD(L5)	-0.5249	-0.1837	0.1929	-16.8	-0.9178	-0.7063	-0.4845	-50.7
CoolD(L2)	0.0013	0.5678	1.1938	76.4	-0.8337	-0.2914	0.1285	-25.3
WarmD(L5)	-1.7085	-1.3392	-0.9888	-73.8	0.2861	0.6383	0.9196	89.3
ρ	0.977	**0.9829**	0.9872	NA	0.977	**0.9824**	0.9867	NA

α	0.0736	**0.1189**	0.1636	NA	0.0737	**0.1193**	0.1651	NA

406

407 3.1.2 Model 2

408 Table 6 (right) summarizes the results of Model 2. The 95% credible intervals do not
409 contain a value of 0, indicating that all the covariates exhibit influential relationships with DENF
410 risk at the neighborhood level in Cali between January 2015 and December 2016. The spatial
411 autocorrelation value of 0.98 indicates that there is very strong spatial dependence of the data
412 after adjusting for covariate effects. The temporal autocorrelation value of 0.11 suggests that
413 there is some presence of temporal dependence of the data after adjusting for covariate effects.
414 Therefore, DENF risk in Cali at the neighborhood level is influenced by DENF rates and
415 covariates in surrounding neighborhoods and time periods (weeks). The DIC (66,964.16) is
416 slightly lower than Model 1 (DENF with no lags – DIC = 67,055.98). In general, the lagged
417 weather variables in Model 2 shrunk the confidence intervals of the coefficients (most notably
418 for average temperature and Days Temp Max); which decreases the uncertainty of our model's
419 risk estimates.

420 Table 6 (right) also shows relative risk estimates of DENF in Cali between January 2015
421 and December 2016. The results suggest a 7.6% increase in DENF risk for PC1; a 3.9% increase
422 for PC2 (negative relationship [decreased risk] in Model 1); a 19.8% increase for proximity to
423 plant nurseries; a 11.8% increase for proximity to tire shops; a -16% decrease for population
424 density; a 12.9% decrease for proximity to rivers/ravines; a 30% increase for tree density; a
425 25.2% decrease for average temperature; a 125.1% increase for days with maximum temp. > 32
426 °C; an 85% increase for relative humidity range; a 91.2% decrease for total rainfall; a 50.7%
427 decrease for total rain days; a 25.3% decrease for cool days; and a 89.3% increase for warm
428 days. The negative to positive relationship between DENF and PC2 observed when comparing

Models 1 and 2 is difficult to interpret. This could be due to the lagged weather variables affecting the posterior estimates. The magnitude of PC2 (low RR) is much lower than the other independent variables, therefore, we hypothesize that people that spend more time at home (PC2) may or may not be more susceptible to DENF and further investigation is required.

3.1.3 Mapping the posterior estimates of DENF

Figure 3 provides maps of the temporal cross-sections of Model 2 posterior values for each neighborhood of DENF rates (per, 1,000) in Cali between 2015 and 2016. The weekly estimates were aggregated by month for visualization purposes – January 2015, July 2015, December 2015, January 2016, July 2016, and December 2016, respectively.

[Insert] Figure 3. Temporal cross-sections of model 2 posterior values for each neighborhood of DENF rate (per 1,000) in Cali.

When comparing the six temporal cross-sections, July 2016 experienced the highest DENF risk (estimated posterior mean values) after accounting for the 14 covariates (including the lagged weather variables). Interestingly, some locations with high rates of DENF are classified as middle (3 or 4) or high strata (5 or 6). These middle and high strata neighborhoods are adjacent to low strata neighborhoods (1 or 2), which suggests that there is spatial-temporal dependence between them. In other words, there is evidence that middle and high strata neighborhoods are at higher risk when surrounded by lower strata neighborhoods after accounting for the covariates in the models. Some of the highest proportion of cases were observed in the eastern portions of Cali (now shown here), but also include some of the highest and most densely populated neighborhoods of the city. After computing rates per 1,000 persons (Figure 3), the eastern portions of Cali (which include some of the poorest neighborhoods) have lower reported rates of DENF than central, southern, and western regions of Cali.

4. Discussion

This study is the first of its kind to model space-time risk at the neighborhood- and weekly- levels of DENF across two years of disease surveillance data; while also incorporating temporally lagged weather variables in a ST-CAR approach. Coupling the lagged weather variables with the spatial covariates of DENF risk, the models include neighborhood-level effects explaining where and why certain locations are more at-risk than others. A quintessential spatiotemporal model decomposes the variability in the outcome in large scale variations (the mean function) and small-scale variation (the spatiotemporal random effects)[22]. Independent variables were used to characterize large-scale variations, while spatiotemporal autocorrelation was used to characterize small-scale variations. The lagged independent variables modified the large-scale variations and for this data it seems they have no effect on small scale variations. The predictive power of the models remains the same, very close DIC values (see Table 6). That is why we are seeing quite robust estimates of spatial autocorrelation parameters in both models. There are many key findings that warrant further investigation and explanation.

4.1 Influence of Socioeconomic and Environmental Factors

First, there is very strong evidence that there is both spatial and temporal dependence between DENF risk and the significant covariates for adjacent neighborhoods in Cali. Although DENF had a much lower temporal autocorrelation (value of 0.11 for both Models 1 and 2), this can be explained by the distribution of cases between 2015 and 2016 – there were three distinct peaks, but DENF remains a persistent threat due to the four serotypes of the virus. The very strong spatial autocorrelation values (although extremely high) for DENF suggest that outbreaks in adjacent neighborhoods are strongly related (i.e. living next to a neighborhood with high cases will strongly influence DENF risk and cases in your neighborhood of residence).

When examining the results of the three socioeconomic covariates (PC1, PC2, and population density), the increased risk of DENF for PC1 is an interesting finding. This corroborates with Delmelle et al. (2016)[30], who suggest that in the southern part of Cali, houses are typically bigger with relatively larger yards, which may provide a suitable habitat for *Aedes* to breed. Neighborhoods with a high proportion of people in the PC1 category (e.g. employed, older, more educated) are also typically adjacent to middle or lower strata neighborhoods (with the exception of the extreme South), which also may increase the risk of disease due to the very strong evidence of space-time dependence between the locations, as suggested by the models. An increased risk of DENF was reported for neighborhoods with higher proportion of individuals in the PC2 category (i.e. work from home and students). This finding corroborates with strong evidence that *Aedes* proliferates in and around homes[57,58,59]; and it has also been found that cases can substantially decline if *Aedes* trap interventions are put in place in at-risk communities[60].

Another unexpected result was the negative relationship between population density and DENF. One explanation can be that some of the densely populated neighborhoods in the eastern part of Cali have a high concentration of Afro-Colombian population, which has been suggested to be less susceptible to the viruses[61,62]. Furthermore, there is evidence that shows that low density areas with poor infrastructure may have increased *Aedes* presence[63] and DENF's complex immunology and the herd immunity resulting after infection from the viruses[64] may have contributed to these patterns. Amongst other factors, high density of populations may not necessarily be a main risk factor of VBD transmission[65]. While increases in population and urbanization will undoubtedly increase risk of VBD transmission, the true effect of population density may vary at fine spatial levels (e.g. neighborhoods). Public health authorities typically

carry out fumigation and education programs in neighborhoods with higher population densities, which may result in a lack of targeted interventions in less dense areas with *Aedes* populations (e.g. sewers, green areas, etc.). Vector control efforts in Cali include storm sewer control, spraying, use of guppy fish, visits to health facilities and homes, and community educational campaigns[35].

Closer proximity to plant nurseries, tire shops, and higher tree density all exhibited an increased risk of DENF. Plant nurseries and tire shops are common breeding grounds of *Aedes*, thus neighborhoods within close proximity are generally at a higher risk of disease transmission. Tree density may also be a significant risk factor of *Aedes* presence since studies have shown that high tree shade density stimulates breeding; and tree holes are suitable water containers where *Aedes* have been found in abundance[67,68].

Closer proximity to rivers and ravines (i.e. any moving bodies of water) resulted in significantly lower risk of DENF. *Aedes* require stagnant water as a breeding ground, therefore, the flowing water of a river or ravine would prove to be an unsuitable habitat for the mosquitoes. Although flooding events during the rainy season could create stagnant water sources surrounding the rivers, however, floods may also act as a disruptive force on *Aedes* habitat by flushing out their breeding sites and eggs[69,70]. Further research using remote sensing techniques (such as flow analysis) could provide insight to areas prone to stagnant water.

4.2 Influence of Weather Factors

In general, the use of optimally lagged weather variables shrunk the confidence intervals about the mean model coefficients and relative risk estimates. Specifically, the individual relationships between each lagged weather covariate and disease risk became either consistently positive or consistently negative (except for average temperature). Moreover, since the optimal

522 lags were different among the weather covariates, our results imply that individual covariates
523 impact different stages of the vector lifecycle (see Table 5). Given that such relationships could
524 inform future space-time modeling and mitigation efforts, the most likely physical connections
525 between local weather conditions and the *Aedes* lifecycle (Tables 4 and 5) are discussed in
526 greater detail based on our Model-2 results (Table 6).

527 Variables with an optimal 5-week lag (Tavg, DTRmax, RainD, WarmD) are most
528 influential on larval development. Both DTRmax and WarmD exhibit the expected positive
529 relationship (Table 5) and large predictive importance based on relative risk estimations (Table
530 6), while RainD exhibits the expected negative relationship with moderate importance. Despite
531 Tavg having an unexpected negative relationship with DENF, its predictive importance is
532 relatively small. Five weeks before above-average DENF rates, the weather is often
533 characterized by multiple days with short-lived rain showers (RainD is above average, its
534 correlation with DENF is negative, and the regression coefficient is negative), yet each day
535 experiences sufficient sunshine to allow the daily maximum temperature to exceed 32°C
536 (WarmD is above average, its correlation with DENF is positive, and the regression coefficient is
537 positive).

538 The short-lived rain showers also induce evaporative cooling that lowers the daily
539 minimum temperature and increases the daily temperature range (DTRmax is above average, its
540 correlation with DENF is positive, and the regression coefficient is positive), leading to slightly
541 cooler, but above-average daily mean temperatures (Tavg remains above average, its correlation
542 with DENF remains positive, but the regression coefficient is slightly negative and the relative
543 risk is small). Overall, regular rainfall combined with average to above-average temperatures

544 produce numerous stagnant pools within a favorable thermal environment for prolific larval
545 development.

546 Variables with an optimal 3-week lag (RainT and RHrng) are most influential on the
547 gonotrophic cycle. Both RainT and RHrng exhibit the expected relationships (Table 5) with
548 similar moderate levels of predictive importance (Table 6). Weather conditions three weeks prior
549 to above-average DENF rates are often characterized by minimal rainfall (RainT is below
550 average, its correlation with DENF is negative, and the regression coefficient is negative) and
551 clear skies, which allows the relative humidity to fluctuate between small daytime values and
552 large nighttime values (RHrng is above average, its correlation with DENF is positive, and the
553 regression coefficient is positive). Overall, the relatively dry conditions maximize solar heating,
554 minimize evaporative cooling, and promote the warm temperatures most favorable for Aedes
555 feeding.

556 Finally, variables with an optimal 2-week lag (CoolD) are most influential on the
557 gonotrophic cycle and extrinsic incubation. Specifically, CoolD exhibits the expected negative
558 relationship (Table 5), but its relative importance is small and roughly equivalent to Tavg.
559 Weather conditions two weeks before above-average DENF rates often exhibit above-average
560 temperatures (CoolD is below average, its correlation with DENF is negative, and the regression
561 coefficient is negative); whereby, the warmer temperatures will accelerate both vector feeding
562 and viral replication within the vector, which increases the potential for transmission to humans.

563 Overall, such consistent multi-lag relationships reinforce the idea that DENF outbreak
564 dynamics are dependent on a complex combination of weather conditions 2-5 weeks prior
565 (Eastin et al. 2014). Careful monitoring of weather conditions within this time window could
566 optimally inform any sub-seasonal DENF mitigation efforts. Moreover, it should be noted that a

moderate El Niño occurred during our 2015-2016 study period[71] and there is strong evidence that major DENF epidemics are more severe during El Nino events[20,72]. Therefore, any sub-seasonal mitigation efforts should also account for inter-seasonal climate variability.

4.3 Limitations

Despite the strengths and contributions of this research, there are notable limitations and areas of future work that is worth discussing. First, the underreporting of cases and unmatched addresses during the geocoding process likely undermines the true burden of DENF. Underreporting is also a major issue in the low strata neighborhoods and also not uniform across the city, while surveillance systems can improve the identification of risk factors throughout the city[73]. Second, the socioeconomic and demographic data was a mix from the Colombian National Census and 2010 population estimates. Colombia recently administered a new national census (the first since 2005) but is currently unavailable. Using 2005 and 2010 data for this study will bias the results, but the neighborhood classifications (strata) mostly remained unchanged. The uncertainty resulting from using outdated census data is a common limitation found in many studies in Latin America and developing countries. Several articles examining patterns of dengue fever in Colombia have recognized outdated population census being a critical issue that could affect the findings of their research[74-79]. Until more recent census are available, different population growth models could address this issue, or relying on disaggregated population projection, using dasymetric mapping[80,81]. Third, including vector surveillance data (presence/absence) in each neighborhood would improve the accuracy of the relative risk estimates[17]. Fourth, the spatial weight matrix only considered adjacent neighborhoods as "neighbors", we recognize that individual activity spaces expand far beyond locations nearby their home. Future research can implement different spatial and temporal weight matrices for

sensitivity analysis purposes. Fifth, the weather conditions and severity of outbreaks for DENF varied between 2015 and 2016, which may have affected the model results. Future work can disaggregate the years and run two separate models for further examination. Sixth, the space-time patterns of the DENF outbreaks did not exhibit much seasonality, which is likely due to only using two years of data. Further work can utilize 5-10 years of DENF and weather data to detect potential seasonal patterns of the epidemics. Finally, weather variability is represented by a single weather station (and thus limited to the temporal domain). Future work would benefit from multiple weather stations that can document spatial variability across the region.

4.4 Opportunities

Chikungunya (CHIK) and Zika are transmitted by the same vector (*Aedes*), and further investigation can develop a multivariate space-time CAR model to examine which neighborhoods are at higher risk for one disease, two diseases, or all three concurrently. Multivariate space-time (MVST) approach in CAR modeling is still in its infancy stages[24] and the development of such models can more accurately examine and compare the co-occurrence of diseases transmitted by the same vector. A long-term goal is to develop a multi-parameter early warning system (EWS) that informs public health officials and motivates effective vector surveillance and control measures. The space-time models and methods described herein represent progress toward that goal. However, effective EWS development would require larger and more comprehensive databases (for both robust model development and independent validation) than those currently available. As noted above, an EWS system would benefit from longitudinal information regarding socioeconomic, demographic, and environmental variables combined with spatial information regarding weather variability across the region.

5. Conclusion

A ST-CAR modeling approach was utilized to examine significant socioeconomic, demographic, environmental, and meteorological risk variable of DENF in Cali, Colombia during 2015 and 2016. The temporally lagged weather covariates can significantly estimate when risk of transmission is highest, and the spatial covariates can help explain the differences in disease risk at the neighborhood-level. Adding weather and climate data to a space-time model can improve disease surveillance, especially for VBDs that require specific conditions for transmission to occur. This study demonstrated that there was strong spatial and temporal dependence between adjacent neighborhoods and time periods, which provides strong evidence that DENF transmission are influenced by characteristics and phenomena occurring in surrounding locations. We also provide evidence that DENF is not just a disease of the poor; although risk factors may be higher in neighborhoods of lower socioeconomic status, we have shown that the transmission dynamics of DENF are place- and temporally based. Despite this study being retrospective in nature, the modeling approach can be applied in a contemporary surveillance setting when significant outbreaks have not yet occurred, highlighting at-risk areas to help promote proactive community health, improve public health educational campaigns, targeted interventions. We hope that this research influences further small area space-time analysis, since we support the notion that disease prevention (in general) should start at the neighborhood and community level.

Acknowledgements

The authors would like to thank the editor and anonymous reviewers for their constructive feedback that ultimately improved the quality of this paper.

References

1. World Health Organization, 2014. “WHO Factsheet Vector-Borne Diseases.” Factsheet

Number 387, no. March: 10. Available at: http://www.who.int/kobe_centre/mediacentre/vbdfactsheet.pdf. Accessed December 2, 2019.

2. Unitaid, 2017. Health experts call for new tools to tackle vector-borne diseases. Available at: https://unitaid.org/news-blog/health-experts-call-new-tools-tackle-vector-borne-diseases/#en. Accessed May 13, 2020.

3. Wang H, et al., 2016. Global, Regional, and National Life Expectancy, All-Cause Mortality, and Cause-Specific Mortality for 249 Causes of Death, 1980-2015: A Systematic Analysis for the Global Burden of Disease Study 2015. The Lancet 388 (10053): 1459–1544.

4. Bhatt S, et al., 2013. The global distribution and burden of dengue. Nature 496 (7446): 504-507.

5. Paupy C, et al., 2010. Comparative role of Aedes albopictus and Aedes aegypti in the emergence of Dengue and Chikungunya in central Africa. Vector-Borne and Zoonotic Diseases 10(3): 259-266.

6. Gratz NG, 2004. Critical review of the vector status of Aedes albopictus. Medical and veterinary entomology 18(3): 215-227.

7. Powell JR, Tabachnick WJ, 2013. History of domestication and spread of Aedes aegypti-A Review. Memorias do Instituto Oswaldo Cruz 108: 11-17.

8. Mustafa MS, Rasotgi V, Jain S, Gupta V, 2015. Discovery of fifth serotype of dengue virus (DENV-5): A new public health dilemma in dengue control. Medical Journal Armed Forces India 71(1): 67-70.

9. World Health Organization, 2018. Dengue and severe dengue. Available at: http://www.who.int/newsroom/fact-sheets/detail/dengue-and-severe-dengue. Accessed September 28, 2019.

10. World Health Organization, 2011. Comprehensive guideline for prevention and control of dengue and dengue haemorrhagic fever. Available at: https://apps.who.int/iris/handle/10665/204894. Accessed January 29, 2020.

11. Gubler DJ, 1998. Dengue and dengue hemorrhagic fever. Clinical microbiology reviews 11(3): 480-496.

12. Toan NT, Rossi S, Prisco G, Nante N, Viviani S, 2015. Dengue epidemiology in selected endemic countries: factors influencing expansion factors as estimates of underreporting. Tropical Medicine & International Health 20(7) 840-863.

13. Shepard DS, Undurraga EA, Halasa YA, Stanaway JD, 2016. The global economic burden of dengue: a systematic analysis. The Lancet infectious diseases 16(8): 935-941.

14. Desjardins MR., Whiteman A, Casas I, Delmelle E, 2018. Space-time clusters and co-occurrence of chikungunya and dengue fever in Colombia from 2015 to 2016. Acta tropica 185: 77-85.

15. Kirby RS, Delmelle E, Eberth JM, 2017. Advances in spatial epidemiology and geographic information systems. Annals of epidemiology 27(1): 1-9.

16. Auchincloss AH, Gebreab SY, Mair C, Diez Roux AV, 2012. A review of spatial methods in epidemiology, 2000–2010. Annual review of public health 33: 107-122.

17. Whiteman A, 2018. Socioeconomic Variation and Aedes Mosquitoes: An Examination of Vector-Borne Disease Risk in the Urban Environment (doctoral dissertation, The University of North Carolina at Charlotte).

18. Bates I, et al, 2004a. Vulnerability to malaria, tuberculosis, and HIV/AIDS infection and disease. Part 1: determinants operating at individual and household level. The Lancet infectious diseases 4(5): 267-277.

19. ———, 2004b. Vulnerability to malaria, tuberculosis, and HIV/AIDS infection and disease. Part II: determinants operating at environmental and institutional level. The Lancet infectious diseases 4(6): 368-375.

20. Eastin MD, Delmelle E, Casas I, Wexler J, Self C, 2014. Intra-and interseasonal autoregressive prediction of dengue outbreaks using local weather and regional climate for a tropical environment in Colombia. The American journal of tropical medicine and hygiene 91(3): 598-610.

21. Semenza JC, Suk JE, Estevez V, Ebi KL, Lindgren E, 2012. Mapping climate change vulnerabilities to infectious diseases in Europe. Environmental health perspectives 120(3): 385.

22. Cressie N, Wikle CK, 2015. Statistics for spatio-temporal data. John Wiley & Sons.

23. Wang M, 2018. Spatio-temporal Statistical Modeling: Climate Impacts due to Bioenergy Crop Expansion (doctoral dissertation, Arizona State University).

24. Lee D, Rushworth A, Napier G, 2018. Spatio-temporal areal unit modelling in R with conditional autoregressive priors using the CARBayesST package. Journal of Statistical Software 84(9): 1-39.

25. Freisthler B, Weiss RE, 2008. Using Bayesian space-time models to understand the substance use environment and risk for being referred to child protective services. Substance Use & Misuse 43(2): 239-251.

26. Lawson AB, 2013. Statistical methods in spatial epidemiology. John Wiley & Sons.

27. Sani A, Abapihi B, Mukhsar M, Kadir K, 2015. Relative risk analysis of dengue cases using convolution extended into spatio-temporal model. Journal of Applied Statistics 42(11): 2509-2519.

28. Mukhsar, Sani A, Abapihi B, Cahyono E, 2016a. Construction Posterior Distribution for Bayesian Mixed ZIP Spatio-Temporal Model. International Journal of Biology and Biomedicine 1: 32-39.

29. Mukhsar, Abapihi B, Sani A, Cahyono E, Adam P, Aini Abdullah F, 2016b. Extended convolution model to bayesian spatio-temporal for diagnosing the DHF endemic locations. Journal of Interdisciplinary Mathematics 19(2): 233-244.

30. Delmelle E, Hagenlocher M, Kienberger S, Casas I, 2016. A spatial model of socioeconomic and environmental determinants of dengue fever in Cali, Colombia. Acta tropica 164: 169-176.

31. Gharbi M, Quenel P, Gustave J, Cassadou S, La Ruche G, Girdary L, Marrama L, 2011. Time series analysis of dengue incidence in Guadeloupe, French West Indies: forecasting models using climate variables as predictors. BMC Infectious Diseases 11: 1–13.

32. Barrera R, Amador M, MacKay AJ, 2011. Population dynamics of *Aedes aegypti* and dengue as influenced by weather and human behavior in San Juan, Puerto Rico. PLoS Neglected Tropical Diseases 5: e1378.

33. Gonzalez R, Suarez MF. 1995. Sewers—the principal Aedes aegypti breeding sites in Cali, Colombia. American Journal of Tropical Medicine and Hygiene 53: 160.

34. Kelly-Hope LA, Purdie DM, Kay BH. 2004. Ross River virus disease in Australia, 1886-1998, with analysis of risk factors associated with outbreaks. Journal of Medical Entomology 41: 133-150.

35. Woodruff RE, Guest CS, Garner MG, Becker N, Lindesay J, Carvan T, Ebi K. 2002. Predicting Ross River virus epidemics from regional weather data. Epidemiology 13: 384-393.

36. Ellis AM, Garcia AJ, Focks DA, Morrison AC, Scott TW. 2011. Parameterization and sensitivity analysis of a complex simulation model for mosquito population dynamics, dengue transmission, and their control. American Journal of Tropical Medicine and Hygiene 85: 257–264.

37. Tun-Lin W, Burkot TR, Kay BH. 2000. Effects of temperature and larval diet on development rates and survival of the dengue vector Aedes aegypti in north Queensland, Australia. Medical Veterinary Entomology 14: 31-37.

38. Rueda LM, Patel KJ, Axtell RC, Stinner RE. 1990. Temperature dependent development and

survival rates of Culex quinquefasciatus and Aedes aegypti. Journal of Medical Entomology 27: 892–898.

39. Thu HM, Aye KM, Thein S. 1998. The effect of temperature and humidity on dengue virus propagation in Aedes aegypti mosquitos. Southeast Asian Journal of Tropical Medicine and Public Health 29: 280-284.

40. Azil AH, Long SA, Ritchie SA, Williams CR. 2010. The development of predictive tools for pre-emptive dengue vector control: A study of Aedes aegypti abundance and meteorological variables in North Queensland, Australia. Tropical Medicine and International Health 15: 1190–1197.

41. Fouque F, Carinci R, Gaborit P, Issaly J, Bicout DJ, Sabatier P. 2006. Aedes aegypti survival and dengue transmission patterns in French Guiana. Journal of Vector Ecology 31: 390–399.

42. Yang HM, Marcoris MLG, Galvani KC, Andrighetti MTM, Wanderley DMV. 2009. Assessing the effects of temperature on the population of Aedes aegypti – the vector of dengue. Epidemiology Infection 137: 1188–1202.

43. Scott TW, Amerasinghe PH, Morrison AC, Lorenz LH, Clark GG, Strickman D, Kittayapong P, Edman JD. 2000. Longitudinal studies of Aedes aegypti in Thailand and Puerto Rico: Blood feeding frequency. Journal of Medical Entomology 37: 89-101.

44. Lambrechts L, Paaijmans KP, Fansiri T, Carrington LB, Kramer LD, Thomas MB, Scott TW. 2011. Impact of daily temperature fluctuations on dengue viral transmission by Aedes aegypti. Proceedings of the National Academy of Sciences USA 108: 7460–7465.

45. Watts DM, Burke DS, Harrison BA, Whitmore RE, Nisalak A. 1987. Effect of temperature on the vector efficiency of Aedes aegypti for dengue-2 virus. American Journal of Tropical Medicine and Hygiene 36: 143–152.

46. Reiter P. 2001. Climate change and mosquito-borne disease. Environmental Health Perspectives 109: 141–161.

47. Jetten TH, Focks DA. 1997. Potential changes in the distribution of dengue transmission under climate warming. American Journal of Tropical Medicine and Hygiene 57: 285–297.

48. Fotheringham AS, Charlton ME, Brunsdon C, 1998. Geographically weighted regression: a natural evolution of the expansion method for spatial data analysis. Environment and planning A 30(11): 1905-1927.

49. Fotheringham AS, Crespo R, Yao J, 2015. Geographical and temporal weighted regression (GTWR). Geographical Analysis 47(4): 431-452.

50. City of Cali. 2020. Estratificación Socioeconómica de Santiago de Cali. Available at: https://www.cali.gov.co/planeacion/publicaciones/107322/estratificacion-socioeconomica-de-santiago-de-cali/. Accessed May 7, 2020.

51. Menne MJ, Durre I, Vose RS, Gleason BE, Houston TG, 2012. An overview of the global historical climatology network-daily database. Journal of Atmospheric and Oceanic Technology 29(7): 897-910.

52. O'brien RM. 2007. A caution regarding rules of thumb for variance inflation factors. Quality & quantity 41(5): 673-690.

53. Wold S, Esbensen K, Geladi P. 1987. Principal component analysis. Chemometrics and intelligent laboratory systems 2(1-3): 37-52.

54. Moran PA, 1950. Notes on continuous stochastic phenomena. Biometrika 37(1/2): 17-23.

55. Rushworth A, Lee D, Mitchell R, 2014. A spatio-temporal model for estimating the long-term effects of air pollution on respiratory hospital admissions in Greater London. Spatial and spatio-temporal epidemiology 10: 29-38.

56. Robert C, & Casella G, 2013. Monte Carlo statistical methods. Springer Science & Business Media.

57. Baldacchino F, Caputo B, Chandre F, Drago A, della Torre A, Montarsi F, Rizzoli A, 2015. Control methods against invasive Aedes mosquitoes in Europe: a review. Pest management science 71(11): 1471-1485.

58. Lindsay SW, Wilson A, Golding N, Scott TW, Takken W, 2017. Improving the built environment in urban areas to control Aedes aegypti-borne diseases. Bulletin of the World Health Organization 95(8): 607.

59. Wilson JJ, Sevarkodiyone SP, 2017. Household survey of dengue and chikungunya vectors (Aedes aegypti and Aedes albopictus) (Diptera: Culicidae) in Tirunelveli district, Tamil Nadu, India. Journal of Entomological Research 41(3): 317-324.

60. Lorenzi OD, 2016. Reduced incidence of Chikungunya virus infection in communities with ongoing Aedes Aegypti mosquito trap intervention studies—Salinas and Guayama, Puerto Rico, November 2015–February 2016. MMWR Morb Mortal Wkly 65.

61. Rojas, J.H. 2011. Dengue y dengue grave", Boletines Unidad de Epidemiología, Santiago de Cali. Available from: http://calisaludable.cali.gov.co/saludPublica/2013_Dengue/revista%20dengue_dengue_grave.pdf. Accessed May 7, 2020.

62. Chacón-Duque JC, et al., 2014. African genetic ancestry is associated with a protective effect on dengue severity in colombian populations. Infection, Genetics and Evolution 27: 89-95.

63. Maciel-de-Freitas R, Lourenço-de-Oliveira R, 2009. Presumed unconstrained dispersal of Aedes aegypti in the city of Rio de Janeiro, Brazil. Revista de saude publica 43: 8-12.

64. Schmidt WP, et al., 2011. Population density, water supply, and the risk of dengue fever in Vietnam: cohort study and spatial analysis. PLoS medicine 8(8): e1001082.

65. Feldstein LR, Brownstein JS, Brady OJ, Hay SI, Johansson MA, 2015. Dengue on islands: a Bayesian approach to understanding the global ecology of dengue viruses. Transactions of the Royal Society of Tropical Medicine and Hygiene 109(5): 303-312.

66. City of Cali. 2020. Administración caleña tomará nuevas medidas contra el dengue. Available from: https://www.cali.gov.co/salud/publicaciones/151526/administracion-calena-tomara-nuevas-medidas-contra-el-dengue/. Accessed May 7, 2020.

67. Lian CW, Seng CM, Chai WY, 2006. Spatial, environmental and entomological risk factor analysis on a rural dengue outbreak in Lundu District in Sarawak, Malaysia. Trop Biomed 23(1): 85-96.

68. Mangudo C, Aparicio JP, Gleiser RM, 2015. Tree holes as larval habitats for Aedes aegypti in urban, suburban and forest habitats in a dengue affected area. Bulletin of entomological research 105(6): 679-684.

69. Benedum, CM, Seidahmed, OME, Eltahir, EAB, Marjuzon, N, 2018. Statistical modeling of the effect of rainfall flushing on dengue transmission in Singapore. PLOS Neglected Tropical Diseases 12 (12).

70. Duchet, C, Moraru, GM, Segev, O, Spencer, M, Gershberg Hayoon, A, Blaustein, L, 2017. Effects of flash flooding on mosquito and community dyanmics in experimental pools. Journal of Vector Ecology 42(2): 254-263.

71. Null J, 2019, El Niño and La Niña Years and Intensities. Available at: https://ggweather.com/enso/oni.htm. Accessed December 10, 2019.

72. Vincenti-Gonzalez MF, Tami A, Lizarazo EF, Grillet ME, 2018, ENSO-driven climate variability promotes periodic major outbreaks of dengue in Venezuela. Scientific reports 8(1): 5727.

73. Desjardins MR, Casas I, Victoria AM, Carbonell D, Dávalos DM, EM, Delmelle, 2020. Knowledge, attitudes, and practices regarding dengue, chikungunya, and Zika in Cali, Colombia. Health & Place 63: 102339.

74. Adin A, Martínez-Bello DA, López-Quílez A, Ugarte MD, 2018. Two-level

resolution of relative risk of dengue disease in a hyperendemic city of Colombia. PLOS One 13(9).

75. Casas I, Delmelle E., Delmelle EC, 2017. Potential versus revealed access to care during a dengue fever outbreak. Journal of Transport & Health 4: 18-29.

76. Casas I, Delmelle E, 2019. Landscapes of healthcare utilization during a dengue fever outbreak in an urban environment of Colombia. Environmental monitoring and assessment 191(2): 279.

77. Fuentes-Vallejo M, 2017. Space and space-time distributions of dengue in a hyper-endemic urban space: the case of Girardot, Colombia. BMC infectious diseases 17(1): 512.

78. Hagenlocher M, Delmelle E, Casas I, Kienberger S, 2013. Assessing socioeconomic vulnerability to dengue fever in Cali, Colombia: statistical vs expert-based modeling. International journal of health geographics 12(1): 36.

79. Hohl A, Delmelle E, Tang W, Casas I, 2016. Accelerating the discovery of space-time patterns of infectious diseases using parallel computing. Spatial and spatio-temporal epidemiology 19: 10-20.

80. Linard C, Tatem AJ, 2012. Large-scale spatial population databases in infectious disease research. International journal of health geographics 11(1): 7.

81. Wardrop NA, et al., 2018. Spatially disaggregated population estimates in the absence of national population and housing census data. Proceedings of the National Academy of Sciences 115(14): 3529-3537.

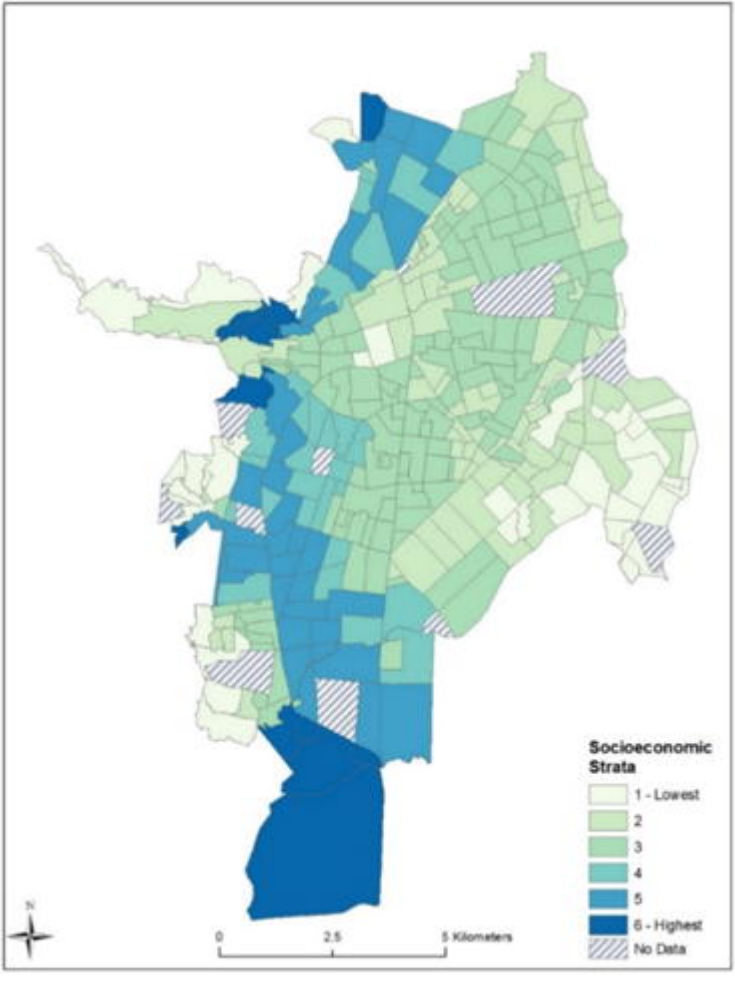
Socioeconomic Strata
1 - Lowest
2
3
4
5
6 - Highest
No Data
N
0
2.5
5 Kilometers

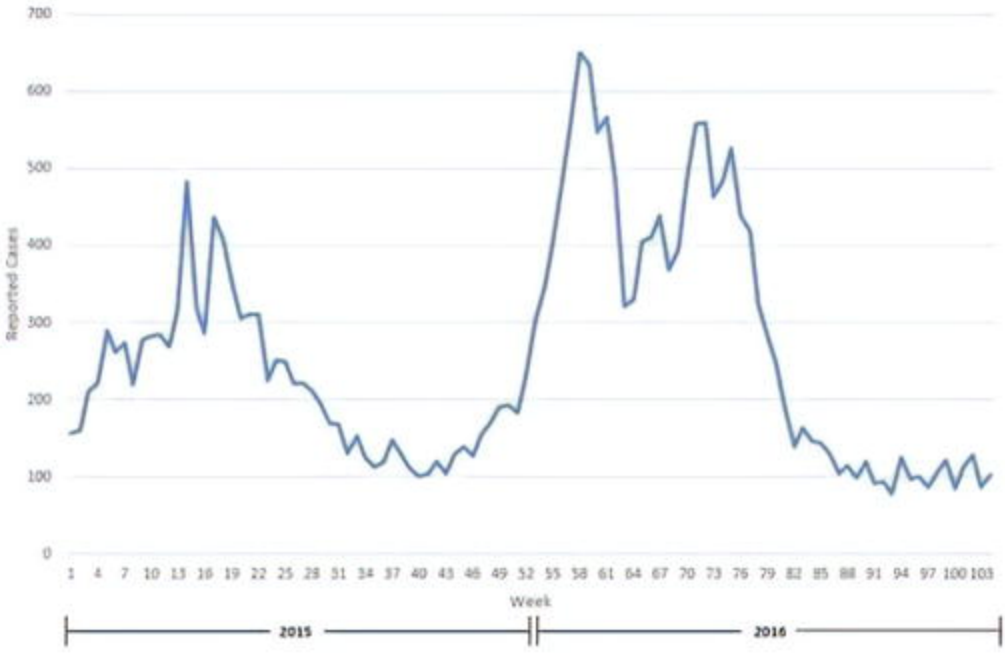
700
600
500
400
300
200
100
0
Reported Cases
1 4 7 10 13 16 19 22 25 28 31 34 37 40 43 46 49 52 55 58 61 64 67 70 73 76 79 82 85 88 91 94 97 100 103
Week
2015
2016

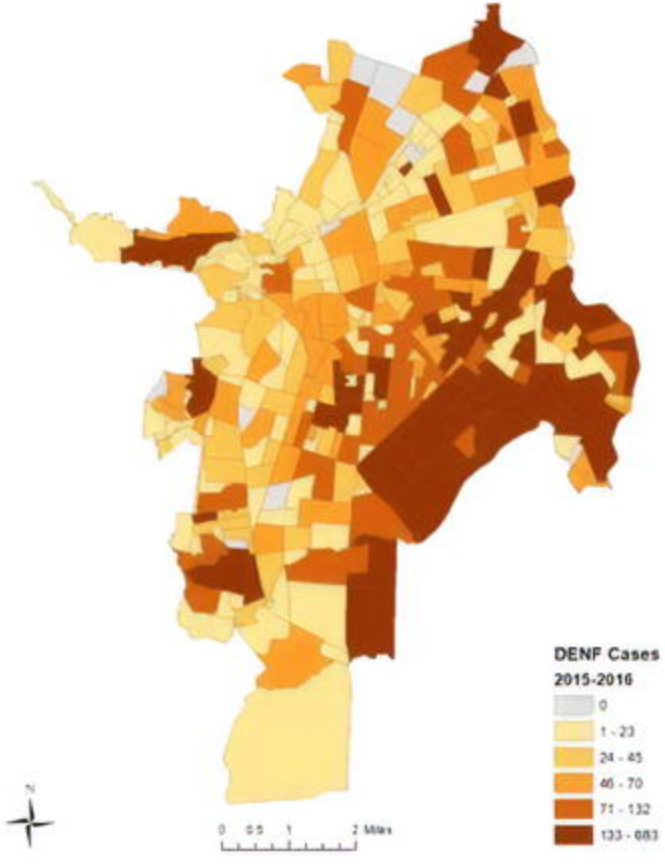
DENF Cases
2015-2016
0
1 - 23
24 - 45
46 - 70
71 - 132
133 - 683
N
0 0.5 1 2 Miles

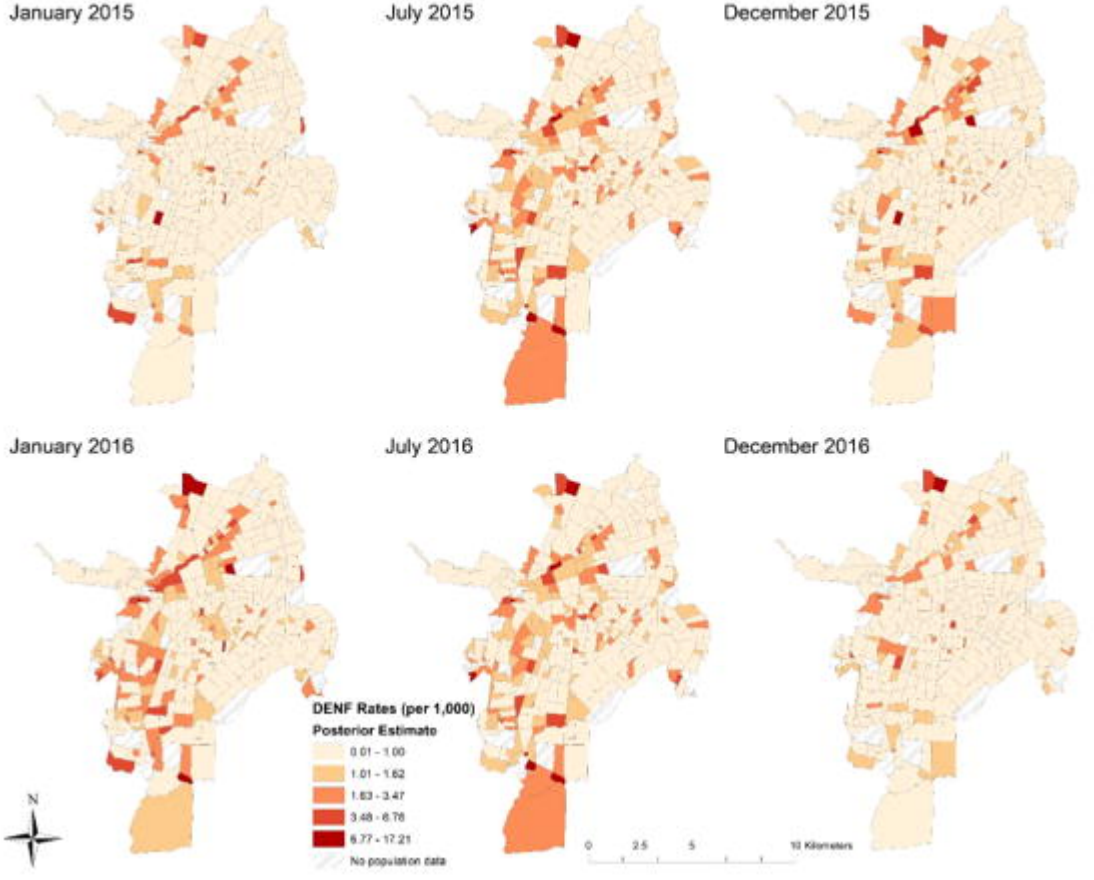
January 2015
July 2015
December 2015
January 2016
July 2016
December 2016
DENF Rates (per 1,000)
Posterior Estimate
0.01 - 1.00
1.01 - 1.62
1.63 - 3.47
3.48 - 6.76
6.77 - 17.21
No population data
N
0
2.5
5
10 Kilometers